

Single-sideband microwave-to-optical conversion in high-Q ferrimagnetic microspheres

Cheng-Zhe Chai^{1,2,†}, Zhen Shen^{1,2,†}, Yan-Lei Zhang^{1,2}, Hao-Qi Zhao^{1,2,‡},

Guang-Can Guo^{1,2}, Chang-Ling Zou^{1,2}, and Chun-Hua Dong^{1,2,*}

¹CAS Key Laboratory of Quantum Information, University of Science and Technology of China, Hefei 230026, P. R. China. and

²CAS Center For Excellence in Quantum Information and Quantum Physics, University of Science and Technology of China, Hefei, Anhui 230026, P. R. China.*

(Dated: November 16, 2021)

Coherent conversion of microwave and optical photons can significantly expand the ability to control the information processing and communication systems. Here, we experimentally demonstrate the microwave-to-optical frequency conversion in a magneto-optical whispering gallery mode microcavity. By applying a magnetic field parallel to the microsphere equator, the intra-cavity optical field will be modulated when the magnon is excited by the microwave drive, leading to microwave-to-optical conversion via the magnetic Stokes and anti-Stokes scattering processes. The observed single sideband conversion phenomenon indicates a non-trivial optical photon-magnon interaction mechanism, which is derived from the magnon induced both the frequency shift and modulated coupling rate of optical modes. In addition, we demonstrate the single-sideband frequency conversion with an ultrawide tuning range up to 2.5GHz, showing its great potential in microwave-to-optical conversion.

I. INTRODUCTION

Electromagnetic waves at microwave and optical frequencies play important roles in information processing and communication systems. However, the quantum information technology based on the most promising superconducting qubits is operated at cryogenic temperature with microwave photons, which cannot achieve long distance communications between qubits. Unlike microwave photons, the optical photon can transmit via low loss optical fibers, making them suitable for long distance communication. Thus frequency conversion between microwave photon and the optical photon has attracted great interest [1–6]. Besides, the energy of single microwave photon is too low to be efficiently detected with a high signal-to-noise ratio. In contrast, converting the microwave photons to optical photons can be detected directly with single-photon detectors. Therefore, it can greatly promote the detection based on the microwave, help to improve the resolution of radar, and maybe realize the quantum enhanced radar system [7]. Recently, such a microwave to optical transducer [6] has

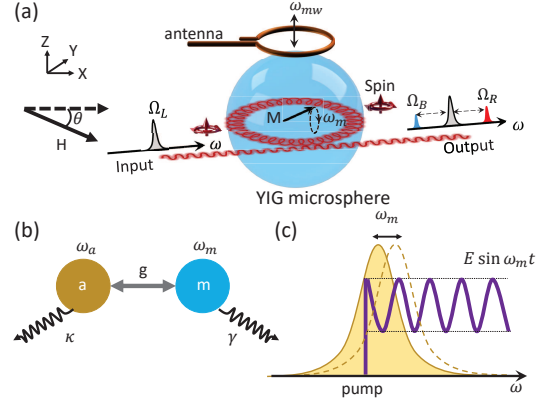


FIG. 1. (a) Schematic of the microwave-to-optical frequency conversion in a YIG microsphere. The bias magnetic field is parallel to the optical path, while the input light excites the WGMs and has an optical spin perpendicular to the propagating direction due to the spin-orbit coupling. The intra-cavity field could be modulated by the dynamic magnetic field via the Faraday effect, and generate two sidebands at the output port. (b) Frequency conversion via the coupling between photon (a) and magnon (m). (c) Illustration of the dispersive magnon-photon coupling as the magnetization induced modulation of the resonant frequency.

been demonstrated in optomechanics, electro-optic interaction, atoms and ions [8–17]. Among these approaches, optomagnonics based on magnon provide an alternative and attractive approach of the coherent microwave-to-optical conversion because of its great frequency tuning range and long coherence time [18–24].

Currently, frequency conversion has been demonstrated in such an optomagnonic system [25–29], where the high Q yttrium iron garnet (YIG) whispering gallery mode (WGM) microcavity was used to enhance the interaction between magnons and photons, and non-reciprocity of the magnetic Brillouin light scattering (BLS) has been observed [27, 30]. However, similar to the Brillouin optomechanical system [31, 32], the triple-resonance condition (the phase matching between pump, signal and a magnetic modes) is required in such system, which may limit the flexibility in choosing the working frequencies and tunability of the frequencies. Therefore, using the great tunability of the magnon and also two-mode magnon-photon coupling mechanism would allow us to achieve transducer that mitigates the above limita-

tions.

In this Letter, a tunable frequency conversion between microwave and photons is realized by the dynamical Faraday effect in a YIG microsphere. The magnetic Stokes and anti-Stokes scattering induced by the dispersive interaction between magnon mode and optical mode can be observed. When the frequency of pump light is resonant with optical mode, the asymmetry of the two sidebands even single sideband (SSB) is observed in our experiment. By changing the direction of the static external magnetic field, we observed both the optical mode resonance frequency shift and modulated coupling efficiency, corresponding to both phase and intensity modulations. Therefore, we deduced that this asymmetry conversion is derived from the phase and intensity modulations induced by the internal magnetization procession. In our experiment, we demonstrated 16 times asymmetry of the two sidebands and the magnon tuning range of 2.5 GHz, corresponding to the tunable frequency conversion with same range. Our results serve as a novel method for the implementation of SSB microwave-to-optical conversion devices.

II. EXPERIMENTAL SETUP AND RESULTS

The principle of the frequency conversion in YIG microsphere is illustrated in Fig. 1(a). The input light couples to the YIG microcavity and excites the WGMs through the high-index prism. The WGMs in microcavity will have a spin along the z direction due to the spin-orbit coupling of light [33–35]. According to our previous work, the spin will be modulated by the magnetization along z direction due to Faraday effect, thus shift the resonant frequency of the WGMs [33]. When applying a magnetic field parallel to the resonator equator, the microwave excites the magnon mode in microcavity by an antenna and causes the procession of the magnetization in microcavity. Therefore, as shown in Fig. 1(c), the resonant frequency of the optical mode in the microcavity will be modulated by the magnetization procession. When an optical pump drives at the optical mode, its amplitude will be modulated and lead to two sidebands at the output as oscillator system, and the Hamiltonian of the system can be written as

$$H = \omega_a a^\dagger a + \omega_m m^\dagger m + g a^\dagger a (m + m^\dagger), \quad (1)$$

where a (a^\dagger), m (m^\dagger) are the annihilation (creation) operators for optical mode and magnon mode, respectively. g is the magneto-optical coupling strength, and ω_a and ω_m are the frequency of the optical mode and magnon mode, respectively. Different from the previous experiment based on triple-resonance condition [25–28], only one optical mode and one magnon mode are participated in the magneto-optical interaction, as shown in Fig. 1(b). Therefore, the interaction between photon and magnon

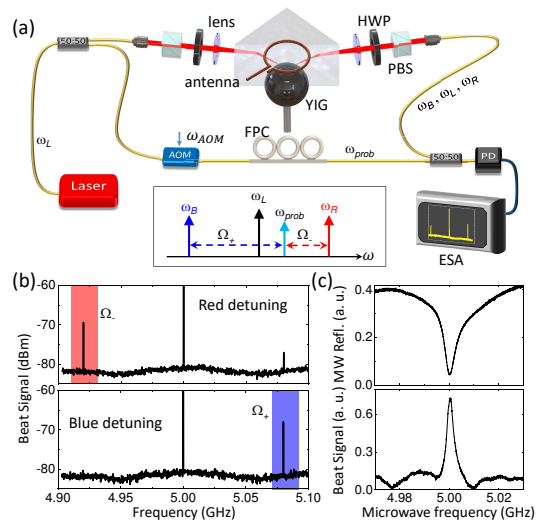


FIG. 2. (a) Schematic of experimental setup. A tunable laser is separated into two beams by an optical fiber splitter. One beam excites the WGMs by prism coupling, which would generate two sidebands at output and then combine another beam as the local oscillator (LO) shifted by an acousto-optic modulator (AOM). PBS: polarization beam splitter. HWP: half wavelength plate. FPC: fiber polarization controller. PD: photon detector. ESA: electric spectra analyzer. Inset: Spectral position of the pump laser, the sidebands and the probe laser as the local oscillator. (b) The detected beat signal when the optical pump at red and blue detunings, respectively. The Ω_- (Ω_+) corresponding to the sideband signal, which is higher (or lower) than the optical pump. (c) Microwave reflection and the generated beat signal as a function of the microwave frequency.

in our experiment is similar to the two mode interaction in optomechanical system [36]. Considering the great tunability of the magnon, a larger operating frequency transducer could be obtained than previous research in optomagnonic system.

Figure 2(a) is the schematic of our experimental setup. A tunable diode laser is separated into two laser beams by an optical fiber splitter. One beam excites the WGMs by the rutile prism, and would generate two sidebands due to the interaction between the magnons and photons. Another laser beam is shifted with frequency of +80MHz by an acousto-optic modulator (AOM) as the local oscillator (LO) to measure the sidebands through heterodyne measurement, as shown in the inset of Fig. 2(a). Two laser beams are combined with the beam splitter and sent a 12 GHz high-speed photon detector followed by a microwave amplifier and a spectrum analyzer. In our experiment, the radius of the YIG microsphere is about 400 μm . Two sets of polarization beam splitters and half-wave plates are used to control the polarization of the system. One is for exciting the different polarized WGMs, and another one is for verifying that the polarization of the generated sideband signal, which is consistent with the pump light. And a fiber polarization controller is

used to make two light paths have the same polarization for optimizing the beat signal. The magnon mode used in the experiment is the uniform mode as known as Kittel mode, whose frequency is determined by $\omega_m = \gamma H$, where $\gamma = 2\pi \times 2.8 \text{ MHz/Oe}$ is the gyromagnetic ratio and H is the external bias magnetic field. The external static magnetic field with intensity of approximately 1780 Oe is parallel to the resonator equator, corresponding to the magnon frequency of approximately 5 GHz , and the Kittel mode is excited by an antenna placed above the YIG microsphere, with the microwave power is amplified up to about 500 mW .

The pump laser with frequency of ω_L modulated by the dynamic Faraday effect through the YIG microcavity will be scattered to two sidebands (ω_R and ω_B). The LO beam has a $+80 \text{ MHz}$ frequency shift with respect to the pump laser. As a result, the sideband signal ω_R (or ω_B) is measured through the beat signals Ω_- (or Ω_+) in spectrum analyzer, as shown in Fig. 2(b). The typical results are measured when the optical pump has a red (or blue) detuning from the optical mode set equal to the magnon frequency, which indicate the Anti-Stokes (or Stokes) scattering. Figure 2(c) shows the microwave reflection and the generated beat signal (Ω_-) as a function of the microwave frequency via a vector network analyzer (VNA). The beat signal shows a resonant characteristics and correlates to the magnon mode which verified the participation of the magnon in the frequency conversion process.

When the pump laser is scanning through the cavity modes, the typical transmission is shown in Fig. 3(a). The dotted line is Lorentz fitting, corresponding to the loaded Q factor of 4.7×10^5 . Figure 3(b) shows the converted signals (Ω_- or Ω_+) obtained with the same optical mode by scanning the pump laser. When the pump laser is red detuning with magnon frequency, the sideband ω_R is resonant with the optical mode and another sideband ω_B is far detuned, thus generate the fairly strong sideband ω_R in optical spectrum, the anti-Stokes scattering dominant at this situation. Therefore, the signal of Ω_- is only observed. To the contrary, the signal of Ω_+ is only observed when the pump laser is blue detuning. Especially, when the pump laser is resonant with optical mode, the modulation of optical resonant would induce two sidebands, as shown both obvious the signal of Ω_- and Ω_+ . Therefore, the signal of Ω_- and Ω_+ has the similar shape just with a magnon frequency shift.

Surprisingly, when the pump laser is resonant with optical mode, the two sidebands signals are asymmetric in Fig. 3(b), in contrast to the symmetric sidebands reported in the dispersively coupled optomechanical systems [37, 38]. To investigate the physical mechanism for this novel SSB phenomenon, Fig. 3(c) shows the optical transmission with changing the magnetic field direction, corresponding to the magnetic field direction changed with the microwave signal. The angle θ between the mag-

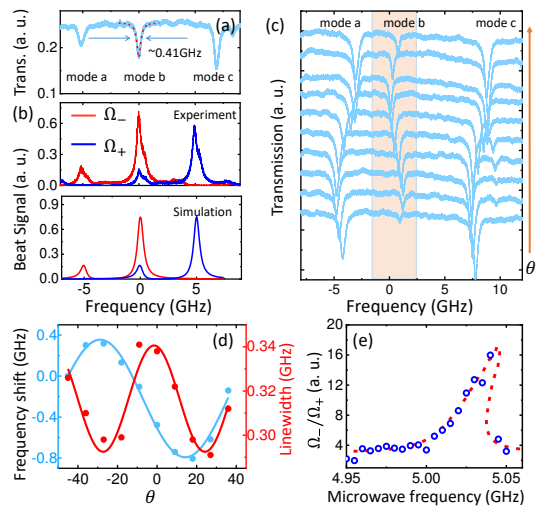


FIG. 3. (a-b) Optical pump transmission and the generated optical signal as a function of pump laser frequency. The experimental results are agreed well with the numerical calculations. (c) Transmission as a function of the input light frequency with different bias magnetic field direction. (d) The frequency shift and linewidth of the optical mode as a function of the bias magnetic field direction from (c). (e) Ω_-/Ω_+ ratio as a function of the input microwave frequency, the red dotted line represents the fitting result when considering the thermal effect of magnon.

netic field direction and the resonator equator is changed from the -45° to 40° . Especially, the transmission of the target optical mode for the efficient frequency conversion has the obvious change during the adjustment, as shown in the gray region of Fig. 3(c), while the transmission of other optical modes have no obvious change during the process. These results indicate that the changed magnetization direction of the YIG sphere could significantly change the coupling strength of the target resonance mode with near-field coupler. Figure 3(d) further shows the resonant frequency and linewidth as a function of the θ . It indicates that both the resonant frequency and linewidth of the optical mode could also be modulated by the dynamic magnetic field and the two modulations have a phase difference $\sim \pi$, corresponding to novel magnon-photon coupling that induces out-of-phase dispersive and dissipative modulations. Similar to the optical SSB modulator [39], such out-of-phase phase modulation (frequency) and intensity modulation (coupling strength) eventually leads to the SSB microwave-to-optical conversion.

To consider the optical mode owning two modulations with the dynamic magnetic field induced by the microwave, one is frequency modulation $ga^\dagger a(m + m^\dagger)$ shown in Eq.(1), and another one is coupling strength modulation which $\kappa_{a,1}$ could be expressed as $\kappa_{a,1}[1 + A(m + m^\dagger)]$, where A is the modulation coefficient of the coupling strength. The coupled-oscillator equations in

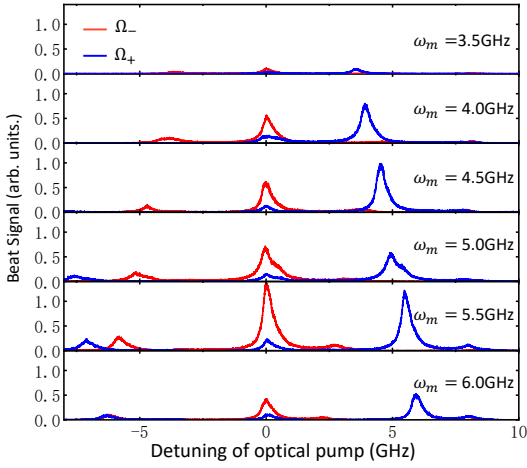


FIG. 4. The converted signal as a function of pump laser frequency with different magnon frequencies by changing magnetic field.

interaction picture are then rewritten as

$$\begin{aligned} \frac{da}{dt} = & [i\Delta_a - \frac{\kappa_a}{2}]a - iga(me^{-i\omega_m t} + \text{H.c.}) \\ & + \sqrt{\kappa_{a,1}} [1 + A(me^{-i\omega_m t} + \text{H.c.})/2] \sqrt{\frac{P_L}{\hbar\omega_L}}, \end{aligned} \quad (2)$$

$$\begin{aligned} \frac{dm}{dt} = & [i\Delta_m - \frac{\kappa_m}{2}]m - iga^\dagger ae^{i\omega_m t} + \sqrt{\kappa_{m,1}} \sqrt{\frac{P_{mw}}{\hbar\omega_{mw}}} \\ & + (A\sqrt{\kappa_{a,1}}/2) \sqrt{\frac{P_L}{\hbar\omega_L}} (a - a^\dagger) e^{i\omega_m t}, \end{aligned} \quad (3)$$

where $\Delta_a = \omega_L - \omega_a$ and $\Delta_m = \omega_{mw} - \omega_m$ are the detuning of the optical and the microwave pump, respectively. κ_a , (κ_m) is the decay rate of the optical (magnon) mode. The numerical results are shown in Fig. 3(b). In Fig. 3(b), one can see that the experimental and numerical results are in good agreement which further verify the two modulation on optical mode causes the SSB phenomenon. Further studies have found that when the pumped laser is kept at the near resonance position, the ratio of beat frequency signal between red and blue (Ω_-/Ω_+) sideband changes with different microwave detuning are measured. The magnon frequency is 5 GHz and it is found that the ratio of beat frequency signal has distinct resonant properties, which means the stronger driving force of microwave enhances the precession amplitude of the magnon along the z-axis near the resonator equator, leading to the stronger SSB effect as shown in Fig. 3(e). The resonant frequency in Fig. 3(e) is larger than 5 GHz because of the thermal effect on the magnon [40].

As we know, the external magnetic field can tune the frequency of the magnon, corresponding to the tunable frequency conversion. Figure 4 shows the frequency conversion by only tuning the relevant magnon frequency

from 3.5 to 6 GHz, which range is limited by the permanent magnet we used. It shows that our device has a much larger operation bandwidth compared to the previous scheme [25–28]. Taking the insertion losses into consideration, the power conversion efficiency in our experiment is estimated as 3.62×10^{-6} . Despite the conversion efficiency is lower than that the previous experiment based on triple-resonance condition [25–29], our experiment provides a novel method to realize the SSB frequency conversion between microwave and optical photons. And the conversion efficiency can be improved by introducing a second microcavity to approach the first microcavity, so that the optical mode will split due to strong coupling between two microcavities [10]. The coupling is tunable, and so the splitting of the optical mode can be selected to match the required magnon frequency to achieve the optical pump and sideband signal resonant with the optical mode, allowing for larger frequency conversion efficiency. Besides, scaling down the size of the YIG microsphere to reduce the mode volume, or replace the microsphere with microdisk and use high order magnetic mode to improve the mode overlap, can further improve the conversion efficiency [27, 29, 41, 42].

III. CONCLUSION

We experimentally demonstrate the SSB frequency conversion between microwave and optical photons in a YIG microcavity. By apply the static magnetic field parallel to the resonator equator, the magnetic Stokes and anti-Stokes scattering occurs in YIG microsphere, which resembles the phonon-photon interaction in an optomechanical system. Besides, due to the modulation of both the resonance frequency and external coupling intensity of optical modes, the SSB modulation has been demonstrated in our experiment. Our results provide a novel method to realize the SSB frequency transducer.

FUNDING

The work was supported by the National Key R&D Program of China (Grant No.2020YFB2205801), the National Natural Science Foundation of China (Grant Nos.11874342, 11934012, 61805229, and 92050109), USTC Research Funds of the Double First-Class Initiative (YD2470002002) and the Fundamental Research Funds for the Central Universities. C.-H. Dong was also supported the State Key Laboratory of Advanced Optical Communication Systems and Networks, Shanghai Jiao Tong University, China. This work was partially carried out at the USTC Center for Micro and Nanoscale Research and Fabrication.

DISCLOSURES

The authors declare no conflicts of interest.

* [†]These authors contributed equally to this work; [‡]Present address: Department of Electrical and Systems Engineering, University of Pennsylvania, Philadelphia, PA 19104, USA; *chunhua@ustc.edu.cn

- [1] R. W. Andrews, R. W. Peterson, T. P. Purdy, K. Cicak, R. W. Simmonds, C. A. Regal, and K. W. Lehnert, “Bidirectional and efficient conversion between microwave and optical light,” *Nature Physics* **10**, 321 (2014).
- [2] J. Bochmann, A. Vainsencher, D. D. Awschalom, and A. N. Cleland, “Nanomechanical coupling between microwave and optical photons,” *Nature Physics* **9**, 712 (2013).
- [3] A. Rueda, F. Sedlmeir, M. C. Collodo, U. Vogl, B. Stiller, G. Schunk, D. V. Strekalov, C. Marquardt, J. M. Fink, O. Painter, *et al.*, “Efficient microwave to optical photon conversion: an electro-optical realization,” *Optica* **3**, 597 (2016).
- [4] N. J. Lambert, A. Rueda, F. Sedlmeir, and H. G. Schwefel, “Coherent conversion between microwave and optical photons—an overview of physical implementations,” *Advanced Quantum Technologies* **3**, 1900077 (2020).
- [5] L. Fan, C.-L. Zou, R. Cheng, X. Guo, X. Han, Z. Gong, S. Wang, and H. X. Tang, “Superconducting cavity electro-optics: a platform for coherent photon conversion between superconducting and photonic circuits,” *Science advances* **4**, eaar4994 (2018).
- [6] X. Han, W. Fu, C.-L. Zou, L. Jiang, and H. X. Tang, “Microwave-optical quantum frequency conversion,” *Optica* **8**, 1050 (2021).
- [7] S. Barzanjeh, S. Guha, C. Weedbrook, D. Vitali, J. H. Shapiro, and S. Pirandola, “Microwave quantum illumination,” *Phys. Rev. Lett.* **114**, 080503 (2015).
- [8] A. Vainsencher, K. Satzinger, G. Peairs, and A. Cleland, “Bi-directional conversion between microwave and optical frequencies in a piezoelectric optomechanical device,” *Applied Physics Letters* **109**, 033107 (2016).
- [9] K. C. Balram, M. I. Davanço, J. D. Song, and K. Srinivasan, “Coherent coupling between radiofrequency, optical and acoustic waves in piezo-optomechanical circuits,” *Nature photonics* **10**, 346 (2016).
- [10] M. Soltani, M. Zhang, C. Ryan, G. J. Ribeill, C. Wang, and M. Loncar, “Efficient quantum microwave-to-optical conversion using electro-optic nanophotonic coupled resonators,” *Phys. Rev. A* **96**, 043808 (2017).
- [11] A. P. Higginbotham, P. Burns, M. Urmey, R. Peterson, N. Kampel, B. Brubaker, G. Smith, K. Lehnert, and C. Regal, “Harnessing electro-optic correlations in an efficient mechanical converter,” *Nature Physics* **14**, 1038 (2018).
- [12] Y. Xu, A. A. Sayem, L. Fan, C.-L. Zou, S. Wang, R. Cheng, W. Fu, L. Yang, M. Xu, and H. X. Tang, “Bidirectional interconversion of microwave and light with thin-film lithium niobate,” *Nature Communications* **12**, 4453 (2021).
- [13] T. Vogt, C. Gross, J. Han, S. B. Pal, M. Lam, M. Kiffner, and W. Li, “Efficient microwave-to-optical conversion using rydberg atoms,” *Physical Review A* **99**, 023832 (2019).
- [14] B. T. Gard, K. Jacobs, R. McDermott, and M. Saffman, “Microwave-to-optical frequency conversion using a cesium atom coupled to a superconducting resonator,” *Phys. Rev. A* **96**, 013833 (2017).
- [15] D. Petrosyan, K. Mølmer, J. Fortágh, and M. Saffman, “Microwave to optical conversion with atoms on a superconducting chip,” *New Journal of Physics* **21**, 073033 (2019).
- [16] S. Welinski, P. J. T. Woodburn, N. Lauk, R. L. Cone, C. Simon, P. Goldner, and C. W. Thiel, “Electron spin coherence in optically excited states of rare-earth ions for microwave to optical quantum transducers,” *Physical Review Letters* **122**, 247401 (2019).
- [17] J. R. Everts, M. C. Berrington, R. L. Ahlefeldt, and J. J. Longdell, “Microwave to optical photon conversion via fully concentrated rare-earth-ion crystals,” *Physical Review A* **99**, 063830 (2019).
- [18] A. V. Chumak, V. I. Vasyuchka, A. A. Serga, and B. Hillebrands, “Magnon spintronics,” *Nature Physics* **11**, 453 (2015).
- [19] M. Harder, Y. Yang, B. M. Yao, C. H. Yu, J. W. Rao, Y. S. Gui, R. L. Stamps, and C.-M. Hu, “Level attraction due to dissipative magnon-photon coupling,” *Physical Review Letters* **121**, 137203 (2018).
- [20] Y. Tabuchi, S. Ishino, A. Noguchi, T. Ishikawa, R. Yamazaki, K. Usami, and Y. Nakamura, “Coherent coupling between a ferromagnetic magnon and a superconducting qubit,” *Science* **349**, 405 (2015).
- [21] D. Lachance-Quirion, S. P. Wolski, Y. Tabuchi, S. Kono, K. Usami, and Y. Nakamura, “Entanglement-based single-shot detection of a single magnon with a superconducting qubit,” *Science* **367**, 425 (2020).
- [22] D. Lachance-Quirion, Y. Tabuchi, A. Gloppe, K. Usami, and Y. Nakamura, “Hybrid quantum systems based on magnonics,” *Applied Physics Express* **12**, 070101 (2019).
- [23] S. Viola Kusminskiy, H. X. Tang, and F. Marquardt, “Coupled spin-light dynamics in cavity optomagnonics,” *Phys. Rev. A* **94**, 033821 (2016).
- [24] J. Graf, H. Pfeifer, F. Marquardt, and S. Viola Kusminskiy, “Cavity optomagnonics with magnetic textures: Coupling a magnetic vortex to light,” *Phys. Rev. B* **98**, 241406(R) (2018).
- [25] X. Zhang, N. Zhu, C.-L. Zou, and H. X. Tang, “Optomagnonic whispering gallery microresonators,” *Physical Review Letters* **117**, 123605 (2016).
- [26] A. Osada, R. Hisatomi, A. Noguchi, Y. Tabuchi, R. Yamazaki, K. Usami, M. Sadgrove, R. Yalla, M. Nomura, and Y. Nakamura, “Cavity optomagnonics with spin-orbit coupled photons,” *Physical Review Letters* **116**, 223601 (2016).
- [27] A. Osada, A. Gloppe, R. Hisatomi, A. Noguchi, R. Yamazaki, M. Nomura, Y. Nakamura, and K. Usami, “Brillouin light scattering by magnetic quasivortices in cavity optomagnonics,” *Phys. Rev. Lett.* **120**, 133602 (2018).
- [28] J. A. Haigh, A. Nunnenkamp, A. J. Ramsay, and A. J. Ferguson, “Triple-resonant brillouin light scattering in magneto-optical cavities,” *Phys. Rev. Lett.* **117**, 133602 (2016).
- [29] N. Zhu, X. Zhang, X. Han, C.-L. Zou, C. Zhong, C.-H. Wang, L. Jiang, and H. X. Tang, “Waveguide cavity

- optomagnonics for microwave-to-optics conversion,” *Optica* **7**, 1291 (2020).
- [30] R. Hisatomi, A. Noguchi, R. Yamazaki, Y. Nakata, A. Gloppe, Y. Nakamura, and K. Usami, “Helicity-changing brillouin light scattering by magnons in a ferromagnetic crystal,” *Physical Review Letters* **123**, 207401 (2019).
- [31] C.-H. Dong, Z. Shen, C.-L. Zou, Y.-L. Zhang, W. Fu, and G.-C. Guo, “Brillouin-scattering-induced transparency and non-reciprocal light storage,” *Nature communications* **6**, 1 (2015).
- [32] M. Aspelmeyer, T. J. Kippenberg, and F. Marquardt, “Cavity optomechanics,” *Rev. Mod. Phys.* **86**, 1391 (2014).
- [33] C.-Z. Chai, H.-Q. Zhao, H. X. Tang, G.-C. Guo, C.-L. Zou, and C.-H. Dong, “Non-reciprocity in high-q ferromagnetic microspheres via photonic spin-orbit coupling,” *Laser & Photonics Reviews* **14**, 1900252 (2020).
- [34] K. Y. Bliokh, F. J. Rodríguez-Fortuño, F. Nori, and A. V. Zayats, “Spin-orbit interactions of light,” *Nat. Photonics* **9**, 796 (2015).
- [35] K. Y. Bliokh, D. Smirnova, and F. Nori, “Quantum spin Hall effect of light,” *Science* **348**, 1448 (2015).
- [36] Z. Shen, Y.-L. Zhang, Y. Chen, C.-L. Zou, Y.-F. Xiao, X.-B. Zou, F.-W. Sun, G.-C. Guo, and C.-H. Dong, “Experimental realization of optomechanically induced non-reciprocity,” *Nature Photonics* **10**, 657 (2016).
- [37] T. J. Kippenberg and K. J. Vahala, “Cavity optomechanics: Back-action at the mesoscale,” *Science* **321**, 1172 (2008).
- [38] E. E. Wollman, C. U. Lei, A. J. Weinstein, J. Suh, A. Kronwald, F. Marquardt, A. A. Clerk, and K. C. Schwab, “Quantum squeezing of motion in a mechanical resonator,” *Science* **349**, 952 (2015).
- [39] Ui-Soo Lee, Hyun-Do Jung, and Sang-Kook Han, “Optical single sideband signal generation using phase modulation of semiconductor optical amplifier,” *IEEE Photonics Technology Letters* **16**, 1373 (2004).
- [40] C.-Z. Chai, X.-X. Hu, C.-L. Zou, G.-C. Guo, and C.-H. Dong, “Thermal bistability of magnon in yttrium iron garnet microspheres,” *Applied Physics Letters* **114**, 021101 (2019).
- [41] N. J. Lambert, J. A. Haigh, and A. J. Ferguson, “Identification of spin wave modes in yttrium iron garnet strongly coupled to a co-axial cavity,” *Journal of Applied Physics* **117**, 053910 (2015).
- [42] J. A. Haigh, N. J. Lambert, S. Sharma, Y. M. Blanter, G. E. W. Bauer, and A. J. Ramsay, “Selection rules for cavity-enhanced brillouin light scattering from magneto-static modes,” *Phys. Rev. B* **97**, 214423 (2018).